

ARTICLE

Fluorogenic Substrate [Ala-Pro]²-Cresyl Violet But Not Ala-Pro-Rhodamine 110 Is Cleaved Specifically by DPPIV Activity: A Study in Living Jurkat Cells and CD26/DPPIV-transfected Jurkat Cells

Emil Boonacker, Sjoerd Elferink, Abdennasser Bardai, Bernard Fleischer, and Cornelis J.F. Van Noorden

Academic Medical Center, University of Amsterdam, Department of Cell Biology and Histology, Amsterdam, The Netherlands (EB,SE,AB,CJFVN), and Bernhard Nocht Institute for Tropical Medicine, Hamburg, Germany (BF)

SUMMARY Fluorogenic substrates [Ala-Pro]²-cresyl violet and Ala-Pro-rhodamine 110 have been tested for microscopic detection of protease activity of dipeptidyl peptidase IV (DPPIV) in living cells. DPPIV activity is one of the many functions of the multifunctional or moonlighting protein CD26/DPPIV. As a model we used Jurkat cells, which are T-cells that lack CD26/DPPIV expression, and CD26/DPPIV-transfected Jurkat cells. Ala-Pro-rhodamine 110 is not fluorescent, but after proteolytic cleavage rhodamine 110 fluoresces. [Ala-Pro]²-cresyl violet is fluorescent by itself but proteolytic cleavage into cresyl violet induces a shift to longer wavelengths. This phenomenon enables the simultaneous determination of local (intracellular) substrate and product concentrations, which is important for analysis of kinetics of the cleavage reaction. [Ala-Pro]²-cresyl violet, but not Ala-Pro-rhodamine 110, appeared to be specific for DPPIV. When microscopic analysis is performed on living cells during the first minutes of the enzyme reaction, DPPIV activity can be precisely localized in cells with the use of [Ala-Pro]²-cresyl violet. Fluorescent product is rapidly internalized into submembrane granules in transfected Jurkat cells and is redistributed intracellularly via internalization pathways that have been described for CD26/DPPIV. We conclude that [Ala-Pro]²-cresyl violet is a good fluorogenic substrate to localize DPPIV activity in living cells when the correct wavelengths are used for excitation and emission and images are captured in the early stages of the enzyme reaction. (*J Histochem Cytochem* 51:959–968, 2003)

KEY WORDS

living cell cytochemistry
protease
metabolic mapping
biocomplexity
CD26/DPPIV
Jurkat cells
confocal scanning laser
microscopy
fluorescence microscopy

Now that genomes of species are becoming elucidated and proteomic analyses in health and disease are under way, analysis of functions of proteins is becoming more important than ever (Jessani et al. 2002). Biocomplexity demands functional analysis in living cells and tissues because interactions between macromolecules and post-translational modifications regulate functions of many macromolecules. This is especially true for enzymes, because their activity and/or their ki-

netic parameters often depend on the microenvironment of the enzyme (Swezey and Epel 1986; Jonges et al. 1992; Van Noorden et al. 1997a; Bleeker et al. 2000; Van Noorden 2002). Therefore, metabolic mapping in living cells and tissues and especially of proteolytic enzymes has gained enormous attention in recent years (Haugland 1995; Perham 2000; Sameni et al. 2000; Boonacker and Van Noorden 2001,2002; Miklos and Maleszka 2001; Hahn and Toutchkine 2002; Patton and Beechem 2002).

Various types of synthetic fluorogenic substrates are available for detection of activity of proteases in living cells (for review see Boonacker and Van Noorden 2001). Usually the substrate consists of one or more sequences of amino acids and a leaving group. The amino acid sequence(s) in the substrate de-

Correspondence to: Prof. Dr. C.J.F. Van Noorden, Dept. of Cell Biology and Histology, Academic Medical Center, Meibergdreef 15, 1105 AZ Amsterdam, The Netherlands. E-mail: c.j.vannoorden@amc.uva.nl

Received for publication December 23, 2002; accepted February 19, 2003 (2A5990).

termine(s) to a large extent the specificity for a protease on the basis of interactions between the amino acid sequence and the active site of the enzyme. Specificity of synthetic substrates is obtained by studying variations in the specificity constant on substitutions or alterations of single amino acids in the substrate (Leytus et al. 1983b). Figure 1 shows two examples of fluorogenic substrates to detect dipeptidyl peptidase IV (DPPIV) activity. Substrate specificity is based on the amino acid sequence alanine-proline (Ala-Pro) (Demuth and Heins 1995) and the leaving groups are either cresyl violet (Figure 1A) or rhodamine 110 (Figure 1B). Rhodamine 110 is not fluorescent when amino acids are attached, as it is completely quenched (Leytus et al. 1983a) and becomes fluorescent after proteolytic release, whereas cresyl violet is always fluorescent even when amino acid sequences are attached but fluorescence is shifted to a longer wavelength (Boonacker and Van Noorden 2001). However, the amino acid sequence does not completely determine substrate specificity because intrinsic chemical properties of fluorophores in synthetic substrates may also affect the reactivity of the substrate with the protease (Chase and Shaw 1969; Boonacker and Van Noorden 2001; Lorey et al. 2002). This phenomenon can be due to steric hindrance or to particular chemical properties of the fluorophore. Assay conditions also determine reactivity of a synthetic substrate with the enzyme. When intact cells or tissues are used, homologous proteases

may interfere with the cleavage of the synthetic substrate.

Proline is a unique amino acid because of its cyclic structure. This specific conformation of proline imposes many restrictions on cleavage of peptides and proteins that contain proline. A large series of physiologically important biomolecules contain proline in the penultimate position and their biological properties are highly regulated by this proline motif. Only a limited number of proteases can cleave proline-containing peptides (Yaron and Naider 1993; Demuth and Heins 1995). Until recently, it was believed that CD26/DPPIV was one of the very few proteases that can cleave off a terminal dipeptide from proteins with proline in the penultimate position, but it has been recently shown that this is not the case (Boonacker and Van Noorden 2003). It appeared that a series of DPPIV homologues exist. For example, DPPII acts preferentially at acidic pH (Lojda et al. 1976) and prollyl carboxypeptidase shows similar activity as CD26/DPPIV (Rawlings and Barrett 1996; Sedo and Malik 2001). Recently, it was found that specific inhibitors of post-proline-cleaving proteases cause apoptosis in quiescent lymphocytes independently of CD26/DPPIV. These results lead to the discovery of another proline-specific peptidase, quiescent cell proline dipeptidase (Chiravuri et al. 1999; Underwood et al. 1999). Quiescent cell proline dipeptidase was cloned from a Jurkat T-cell line that lacks CD26/DPPIV expression. The putative active site residues serine, aspartate, and his-

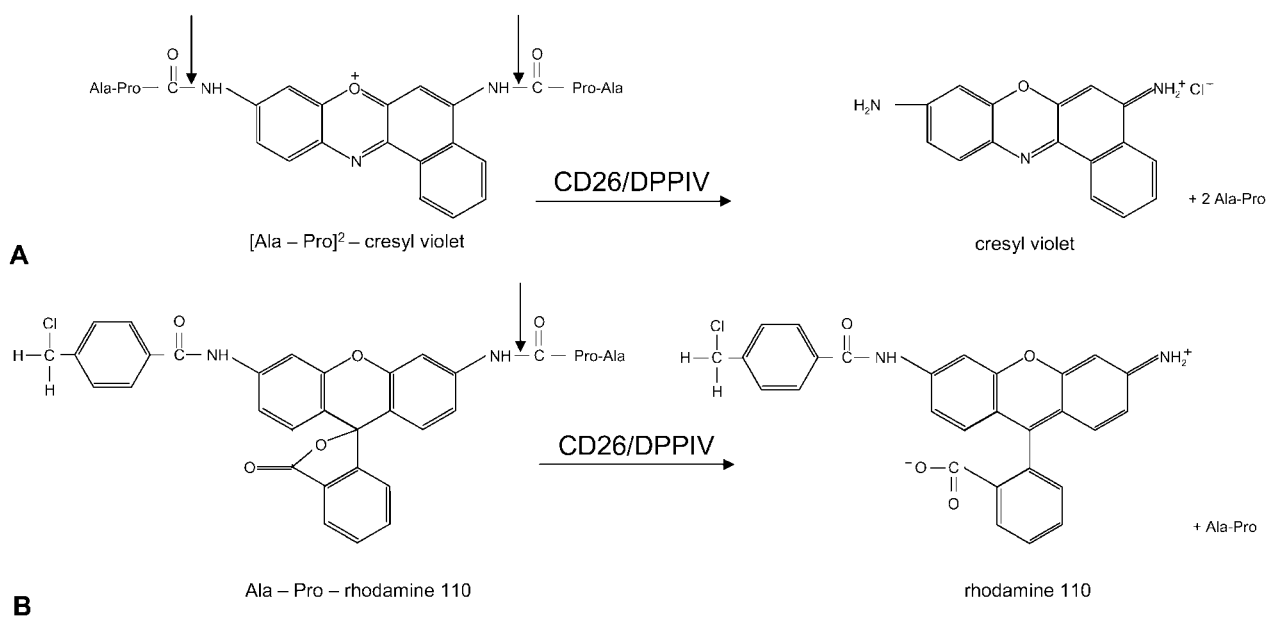


Figure 1 Structural formulas of the bisubstituted [Ala-Pro]²-cresyl violet (**A**) and monosubstituted Ala-Pro-rhodamine 110 (**B**) synthetic substrates and the reaction scheme of their cleavage by DPPIV activity into the products Ala-Pro and cresyl violet (**A**) and rhodamine 110 (**B**), respectively.

tidine of quiescent cell proline dipeptidase shows an ordering of the catalytic triad similar to that in the post-proline-cleaving exopeptidases prolyl carboxypeptidase and CD26/DPPIV (David et al. 1993; Hooper et al. 2001). DPPIV homologues are listed in Sedo and Malik (2001) and in Boonacker and Van Noorden (2003). To study activity of DPPIV and its homologues in a specific manner, the characteristics of fluorogenic substrates have to be known.

In this study we compared the reactivity of two synthetic substrates that contain the same amino acid sequence but different fluorogenic leaving groups, cresyl violet (Van Noorden et al. 1997b) and rhodamine 110 (Leytus et al. 1983a,b; Figure 1), in the analysis of DPPIV activity after purification and in living Jurkat cells lacking CD26/DPPIV and CD26/DPPIV-transfected Jurkat cells (Hegen et al. 1993a,b; Tanaka et al. 1993) to establish to what extent the Ala-Pro-containing substrates are specific for DPPIV. We found that the two substrates show different specificities towards DPPIV-like proteases, depending on the leaving group. [Ala-Pro]²-cresyl violet is specific for DPPIV activity whereas Ala-Pro-rhodamine 110 is not. We concluded that [Ala-Pro]²-cresyl violet is the preferred substrate for microscopic analysis of DPPIV activity in living cells. Because of the highly dynamic character of (enzymatic) processes in living cells and to avoid diffusion of cresyl violet from sites in cells where it is formed, microscopic images have to be taken during the first few minutes of incubation of cells.

Materials and Methods

Jurkat Cell Lines

Jurkat cells (clone E6-1; American Type Culture Collection, Manassas, VA), which lack CD26/DPPIV expression, were used as well as Jurkat cells transfected with CD26/DPPIV (Hegen et al. 1993a,b). This model system enables the determination of specificity of substrates for DPPIV. Clone E6-1 was cultured in Iscove's modified Dulbecco's medium (IMDM; Bio-Whitaker, Walkersville, MD) supplemented with 10% fetal calf serum (FCS), whereas the CD26/DPPIV transfectants were grown in Dulbecco's modified medium supplemented with 10% FCS, containing glutamine (1 mM) and Geneticin G418 (1 mg/ml; Invitrogen, Carlsbad, CA) to maintain the selection for the CD26/DPPIV construct (Hegen et al. 1993a,b; Tanaka et al. 1993). Before DPPIV activity measurements, cells were washed twice in cold PBS. Intact cells were kept on ice before mixing with the incubation media. Suspensions of 4×10^6 cells/ml were used. Permeabilization of cells was performed by ultrasonic treatment (three times, 5 sec each).

Western Blotting and Zymography of DPPIV Activity

To test specificity of substrates, samples containing soluble CD26/DPPIV (sCD26/DPPIV) derived from human seminal fluid were run on polyacrylamide gels and submitted to

Western blotting or were incubated in the presence of a series of synthetic DPPIV substrates. sCD26/DPPIV was enriched by isolating prostasomes from human seminal fluid, as described by Ronquist and Brody (1985). The pelleted prostatic fraction was resuspended in 20 mM Tris-HCl (pH 7.4) containing 1% Triton X-100 for 1 hr at 4°C. Samples were treated ultrasonically three times for 5 sec each. Subsequently, $3 \times$ Laemmli buffer, consisting of 150 mM Tris-HCl (pH 6.8), 30% glycerol, 6% SDS, and 0.3% bromophenol blue, was added and the samples were heated to 37°C for 5 min. Equal amounts of proteins were transferred onto the gels. After electrophoresis at 20 mA per gel at 4°C, gels were washed twice at room temperature (RT) with PBS containing 2.5% Triton X-100 for 30 min to remove SDS.

DPPIV activity was detected with the following substrates: 20 μ M [Ala-Pro]²-cresyl violet (Enzyme Systems Products and Prototek, Livermore, CA; Van Noorden et al. 1997b), 20 μ M Ala-Pro-AFC (Enzyme Systems Products; Smith et al. 1997), or 20 μ M Ala-Pro-MNA (Enzyme Systems Products; Smith et al. 1997) in 100 mM cacodylate buffer (pH 7.4), or 20 μ M Ala-Pro-rhodamine 110 (Molecular Probes, Eugene, OR; Leytus et al. 1983a,b) in 10 mM Tris-HCl buffer (pH 7.5). In the case of Ala-Pro-MNA, a coupling agent was added as well, either 1 mM nitrosalicylaldehyde (Merck, Darmstadt, Germany; Van Noorden and Frederiks 1992) or Fast Blue B (FBB₄; Serva, Heidelberg, Germany; Van Noorden and Frederiks 1992). After 20 min of incubation, DPPIV activity was determined using a STORM Fluor-imager (Molecular Dynamics; Sunnyvale, CA) and Image Quant Software Package (Molecular Dynamics) or, in the case of the chromogenic substrates, scanned on a flatbed scanner using white light.

Samples were also subjected to Western blotting to determine CD26/DPPIV protein expression. Proteins were blotted at 4°C and 100 V to nitrocellulose paper for 1 hr. After washing in PBS containing 0.05% Tween, blots were blocked overnight with 5% BSA in PBS. Blots were incubated with anti-CD26 antibody Ta1 (Central Laboratory for Blood Transfusion; Amsterdam, The Netherlands) at a dilution of 1:100 in the blocking buffer containing 0.05% Tween for 1 hr, then washed twice in PBS containing 0.05% Tween, followed by 1-hr incubation with monoclonal horseradish peroxidase-conjugated goat anti-mouse IgG (Nordic; Tilburg, The Netherlands) in a dilution of 1:200 in blocking buffer. Then blots were washed again in PBS. Finally, after 10 min of incubation with Lumi-Light Western blotting substrate (Roche Diagnostics; Mannheim, Germany), chemiluminescence was detected by the Lumi-Imager (Roche Diagnostics).

Fluorescence Spectra of [Ala-Pro]²-Cresyl Violet Substrate and Cresyl Violet Product

Fluorometric analysis of concentrations of [Ala-Pro]²-cresyl violet and cresyl violet acetate (Enzyme Systems Products) was performed on a LS 50 fluorescence spectrometer (Perkin-Elmer; Gouda, The Netherlands). [Ala-Pro]²-cresyl violet (20 μ M) and cresyl violet acetate (20 μ M) were measured separately and mixed in 1:1 and 1:4 ratios. Excitation was performed at 496 nm and 591 nm and fluorescence emission was monitored at wavelengths ranging from 500 nm to 700 nm.

Thin-Layer Chromatography of [Ala-Pro]²-Cresyl Violet Substrate and Cresyl Violet Product

To demonstrate fluorescent components in batches of substrate and product, separation by thin-layer chromatography (TLC) was performed, using silica gel-coated TLC plates (Merck; Darmstadt, Germany) as the stationary phase and methanol as the mobile phase. Equal amounts of substrate and product molecules were dissolved in methanol and applied to TLC plates. The plates were placed upright in running fluid and ran until the front of the running fluid had reached the end of the plate. The plates were dried and stored for further analysis. Images of the plates were made using white light and a digital camera (Coolpix; Nikon, Tokyo, Japan) to demonstrate the color change from orange to violet as is also observed with the naked eye when living cells are incubated with the substrate in a cuvette. Then the plates were illuminated with UVA light (320–380 nm), and photographed with a UV-blocking filter (>500 nm) using the same camera.

Fluorometric Analysis of DPPIV Activity

Living Jurkat cells and CD26/DPPIV-transfected Jurkat cells were harvested and DPPIV activity was determined by fluorometry. Before DPPIV activity measurements, cells were washed twice in cold PBS. Intact cells were kept on ice before mixing with the enzyme incubation media. Parts of the cells were lysed by ultrasonic treatment three times for 5 sec. Incubations were started at $t=0$ by suspending Jurkat cells or transfected Jurkat cells in prewarmed PBS supplemented with 1.7 mM CaCl₂ and 1 mM MgCl₂ at 37°C containing 0–40 μ M of the DPPIV substrate [Ala-Pro]²-cresyl violet or Ala-Pro-rhodamine 110. Actual amounts of ester bonds that are cleaved are twice as high as that of the free fluorochrome in the case of [Ala-Pro]²-cresyl violet, because two amino acid sequences are spliced off per cresyl violet fluorochrome (Figure 1). Incubations were carried out at 37°C by using prewarmed PBS to which the substrate was added just before the start of the incubation. The cell suspension was kept on ice before the incubation and added 30 sec after the start of recording. For each measurement, 4×10^6 living cells, or its equivalent in cell lysates, were incubated in a final volume of 1200 μ l prewarmed PBS containing 0–40 μ M [Ala-Pro]²-cresyl violet or Ala-Pro-rhodamine 110 substrate. Fluorometric analysis was performed on an LS 50 fluorescence spectrometer under continuous magnetic stirring to keep cells in suspension. Cuvettes with an excitation light path of 1 cm and an emission light path of 4 mm were used. Excitation for cresyl violet was performed at 591 nm with a slit width of 10 nm and emission was detected at 628 nm with a slit width of 10 nm (Boonacker and Van Noorden 2001). Rhodamine 110 was excited at 491 nm with a slit width of 10 nm and emission was detected at 529 nm with a slit width of 10 nm (Boonacker and Van Noorden 2001). Fluorescence was measured continuously during the first 4 min of incubation. Because both synthetic substrates are not completely stable in aqueous solution, a spontaneous small but continuous increase of fluorescence is detected when the substrates are incubated in an aqueous solution. By starting the incubation with the medium containing the substrate only, fluorescence of Ala-Pro-

cresyl violet due to spontaneous formation of product (both cresyl violet and rhodamine 110) was measured. These values were subtracted from fluorescence values obtained after the cells were added to the medium, thus correcting for the spontaneous nonspecific increase in fluorescence. Fluorescence values were plotted against time.

Confocal Microscopic Analysis of DPPIV Activity in Living Cells

Confocal analysis was performed to localize DPPIV-like activity in living Jurkat and transfected Jurkat cells on a Leica SP₂ AOBs confocal microscope (Leica Microsystems; Mannheim, Germany). In case of the use of [Ala-Pro]²-cresyl violet, fluorescence of both substrate and product was analyzed with settings of the AOBs for 488-nm excitation of the substrate and 594-nm excitation of the product. Fluorescence was measured at 515–576 nm and 613–734 nm for substrate and product, respectively. Each focal plane was scanned in a sequential manner in time, xyt, or in volume, xyz, for end-point images. In case of the use of Ala-Pro-rhodamine 110, excitation was performed at 496 nm and emission was measured at 550–580 nm. Living Jurkat cells were incubated on the stage of a confocal microscope in Dulbecco's modified medium containing 0.1 mg/ml Geneticin G418 and 1 mM glutamine and 10% FCS. This medium allowed prolonged incubations for longer periods of time without any significant cell damage. The suspended cells were incubated in 1 ml incubation medium on the microscope stage on a γ -irradiated glass bottom in a poly-L-lysine-coated petri dish (MatTek; Ashland, MA). The nonadherent blood cells tend to stick after a certain period of time to the poly-L-lysine-coated glass bottom. After allowing the cells to adhere for a few minutes, cells were selected in the transmission image mode using white light and brought into focus, and transmission images were made to check whether cells were not moving any more. Then substrate was added by carefully dropping the substrate on top of the cells, preventing the cells to drift out of focus or the field of observation. Then the substrate was added as 10 μ l of a 100 \times concentrated stock solution to the medium. The petri dishes were mounted in the specimen clamp on the stage of the microscope with the use of a circular rubber self-constructed O-ring. This enables the administration of the substrate directly on top of the cells, while the cells can be imaged continuously. The first fluorescence images were captured at 30 sec after the substrate was added in a single focal plane at a rate of 1.8 sec per scan. In total, 200 images were made in 6 min. Sequential scanning was performed to minimize crosstalk.

Results

Reactivity of the various Ala-Pro-containing synthetic substrates with CD26/DPPIV was demonstrated with the use of an enriched fraction of sCD26/DPPIV that was submitted to native gel electrophoresis and Western blotting. Figure 2 demonstrates a similarly stained banding pattern with two major bands of DPPIV activity obtained with all substrates tested. Western blotting after staining with the anti-CD26/DPPIV anti-

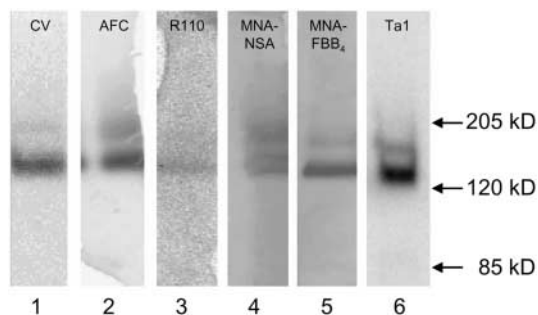
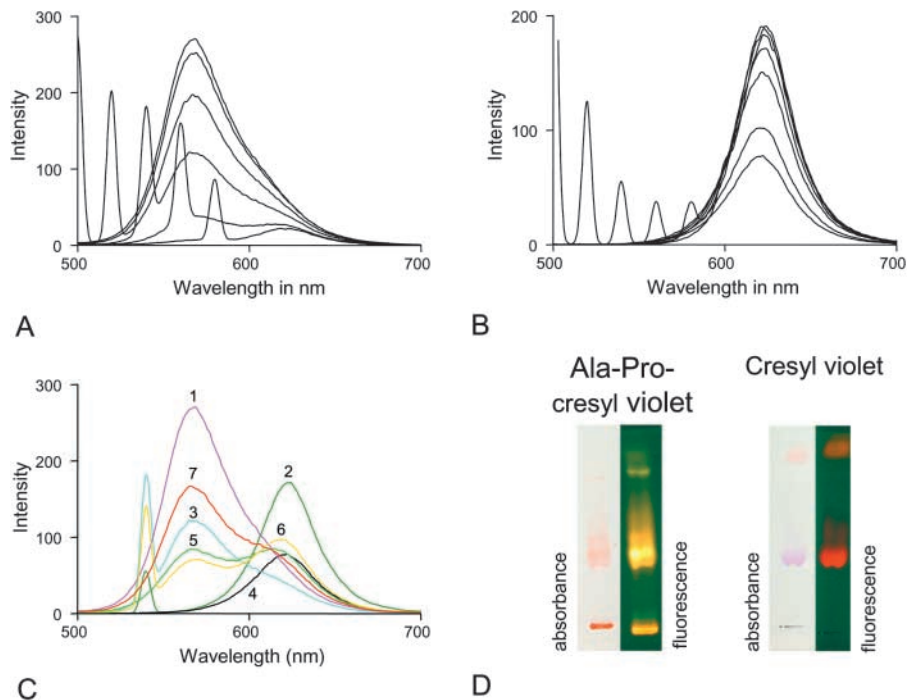


Figure 2 DPPIV activity as detected after gel electrophoresis of sCD26/DPPIV enriched from prostasomes in human seminal fluid with different synthetic substrates for DPPIV (Lanes 1–5) and CD26/DPPIV protein after Western blotting (Lane 6). DPPIV activity is detected in Lane 1 with [Ala-Pro]²-cresyl violet (CV), in Lane 2 with Ala-Pro-AFC (AFC), in Lane 3 with Ala-Pro-rhodamine 110 (R110), in Lane 4 with Ala-Pro-MNA in combination with NSA as coupling agent (MNA-NSA), in Lane 5 with Ala-Pro-MNA in combination with FBB₄ as coupling agent (MNA-FBB₄), and CD26/DPPIV is detected in Lane 6 with an anti-CD26 monoclonal antibody (Ta1). Molecular weight markers are presented at right. Native CD26/DPPIV is located just above the arrow of 120 kD, which is in agreement with the molecular weight of 140 kD of the native protein. Due to the limited number of excitation wavelengths on the storm scanner, emission intensities cannot be directly compared with respect to reactivity.

body shows a similar banding pattern as well (Figure 2). These findings indicate that all substrates identify DPPIV activity and demonstrate the different isoforms of DPPIV/CD26 as they occur in prostasomes. It should be noted that intensities cannot be compared directly due to the limited number of excitation wavelengths available on the scanner used and thus to the more or less optimal excitation of the fluorophores.

To characterize the shift in fluorescence that occurs after proteolytic cleavage of [Ala-Pro]²-cresyl violet into cresyl violet and Ala-Pro dipeptides, emission and excitation spectra were determined for both [Ala-Pro]²-cresyl violet substrate and cresyl violet product separately (Figures 3A and 3B), and in mixtures with different ratios (1:1, 1:4; Figure 3C). Solutions of 20 μM were made of both substrate and product, and emission spectra were determined. When light of 480, 500, 520, or 540 nm was used for excitation, [Ala-Pro]²-cresyl violet showed one emission peak at 570 nm (Figure 3A). When excitation light of 560 or 580 nm was used, emission was at a higher wavelength but insignificant. When light of 480, 500, 520, 540, 560, or 580 nm was used for excitation, the proteolytic product cresyl violet was fluorescent with one emis-

Figure 3 Emission spectra of [Ala-Pro]²-cresyl violet (A) and its cleavage product cresyl violet (B). [Ala-Pro]²-cresyl violet shows maximal absorbance at 488 nm and an emission maximal at 570 nm (A). Cresyl violet shows an absorbance maximum at 591 nm and an emission maximum at 628 nm (B). Both in A and B, spectra were collected using excitation light of 480, 500, 520, 540, 560, and 580 nm. Excitation stray light peaks are present in both figures. Although the spectra are not corrected for excitation light energy, maxima of emission were consequently found at 570 nm for substrate and at 628 nm for product. (C) Mixtures of substrate and product in 1:1 and 1:4 ratios at suboptimal excitation of wavelengths of 480 nm and 540 nm that are available on commercial confocal microscopes. It shows that specific product fluorescence is hard to detect when the wrong excitation is used. 1, Emission spectrum of 20 μM [Ala-Pro]²-cresyl violet when excited at 480 nm. 2, Emission spectrum of 20 μM cresyl violet when excited at 540 nm. 3, Emission spectrum of [Ala-Pro]²-cresyl violet when excited at 540 nm. 4, Emission spectrum of cresyl violet when excited at 480 nm. 5, Emission spectrum of a 1:1 mixture of [Ala-Pro]²-cresyl violet and cresyl violet when excited at 480 nm. 6, Emission spectrum of a 1:4 mixture of [Ala-Pro]²-cresyl violet and cresyl violet when excited at 540 nm. 7, Emission spectrum of a 1:4 mixture of [Ala-Pro]²-cresyl violet and cresyl violet when excited at 480 nm. (D) TLC analysis of [Ala-Pro]²-cresyl violet and cresyl violet. Lane 1 shows the orange-red color of [Ala-Pro]²-cresyl violet substrate as detected by illumination with white light. Lane 2 shows fluorescence of [Ala-Pro]²-cresyl violet substrate as detected with UVA light of 320–380 nm and a longpass filter of >500 nm. Lane 3 shows the deep red color of cresyl violet as detected by illumination with white light. Lane 4 shows fluorescence of cresyl violet as detected with UVA light illumination and a longpass filter.



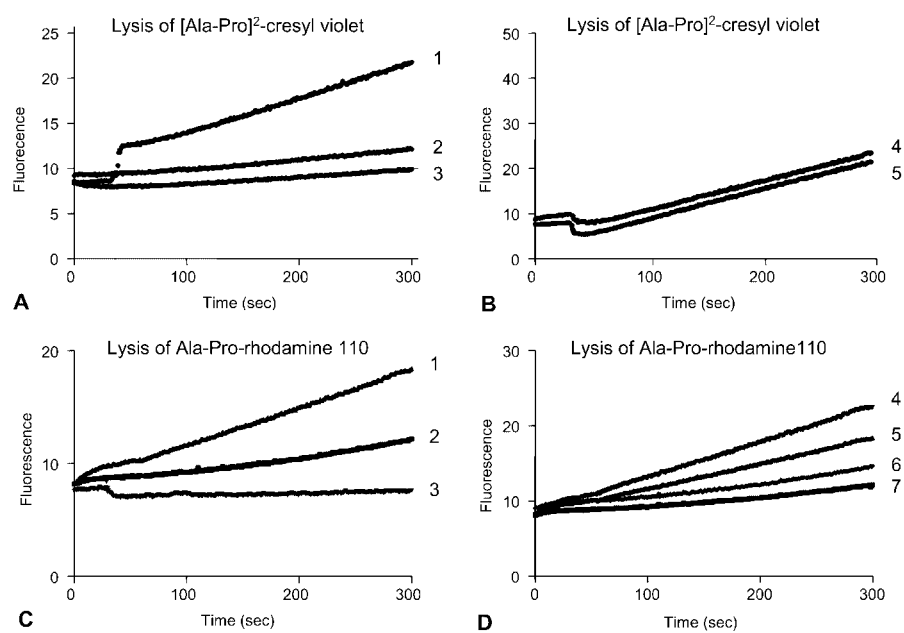


Figure 4 (A) Increase in fluorescence in time at 628 nm after excitation at 591 nm as a measure of production of cresyl violet in a solution of 20 μ M [Ala-Pro]²-cresyl violet in the presence or absence of intact living Jurkat cells lacking CD26/DPPiV and CD26/DPPiV-transfected Jurkat cells. The substrate is not stable in the aqueous medium and cresyl violet is generated in the medium with substrate alone (line 3). Jurkat cells produce a similar increase in fluorescence as the medium with substrate alone (line 2), whereas CD26/DPPiV-transfected Jurkat cells produce significantly higher amounts of fluorescence at 628 nm (line 1). (B) Production of fluorescence in time at 628 nm in intact (line 5) and permeabilized CD26/DPPiV-transfected Jurkat cells (line 4). Permeabilization does not affect the rate of fluorescence production (compare slopes of lines 4 and 5). (C) Increase in fluorescence in time at 529 nm after excitation at 488 nm as a measure of production of rhodamine 110 in a

solution of 20 μ M using Ala-Pro-rhodamine 110 in the presence or absence of intact living Jurkat cells lacking CD26/DPPiV and CD26/DPPiV-transfected Jurkat cells. Ala-Pro-rhodamine 110 alone produces little fluorescence, indicating little instability of the substrate in PBS (line 3), but intact Jurkat cells show a distinct additional increase in fluorescence (line 2), indicating that the rhodamine 110-containing substrate is cleaved by proteases other than DPPiV. CD26/DPPiV-transfected Jurkat cells show a distinctly higher increase in fluorescence (line 1). (D) Production of fluorescence in intact (line 5) and permeabilized CD26/DPPiV-transfected Jurkat cells (line 4) and intact (line 7) and permeabilized Jurkat cells (line 6) using Ala-Pro-rhodamine 110 substrate. Permeabilized cells show higher rates of fluorescence production than intact cells (compare slopes of line 4 and line 5, and slopes of line 6 and line 7).

sion peak only at 628 nm (Figure 3B). Because of the broad fluorescence spectrum of the substrate [Ala-Pro]²-cresyl violet, fluorescence of the product could not be detected specifically when excitation light was used at a wavelength <570 nm because the substrate caused too high levels of background fluorescence (Figure 3C). In practice, substrate concentrations are much higher than product concentrations in cells when initial stages of enzyme reactions are measured. On the other hand, the 570-nm fluorescence of [Ala-Pro]²-cresyl violet substrate can be used to determine amounts of substrate present in both cells and/or incubation medium to enable the determination of kinetics of [Ala-Pro]²-cresyl violet cleavage on the basis of local substrate concentrations and production of cresyl violet. The spectra illustrate that for specific measurement of fluorescence of the cresyl violet product at 628 nm, excitation at 591 nm must be used to avoid interference by fluorescence of [Ala-Pro]²-cresyl violet (Figure 3C). In conclusion, when an excitation wavelength of 591 nm is used, fluorescence at 628 nm is specific for the product. The substrate concentration can be measured using excitation at 488 nm and emission at 570 nm.

Ala-Pro-rhodamine 110 substrate is not fluorescent, whereas the DPPiV reaction product, rhodamine

110, has an excitation peak at 491 nm and an emission peak at 529 nm (Leytus et al. 1983a,b).

Comparison of [Ala-Pro]²-cresyl violet and cresyl violet bands after TLC shows the color shift in both absorbance and fluorescence when the substrate is proteolytically cleaved (Figure 3D). A similar color change is observed when CD26/DPPiV is incubated with the substrate. Specificity of [Ala-Pro]²-cresyl violet and Ala-Pro-rhodamine 110 as substrates for CD26/DPPiV was demonstrated in intact and permeabilized wild-type Jurkat cells and CD26/DPPiV-

Table 1 Kinetic parameters of cleavage of [Ala-Pro]²-cresyl violet (CV) and [Ala-Pro]-rhodamine 110 (R110) by intact and permeabilized Jurkat cells and CD26/DPPiV-transfected Jurkat cells

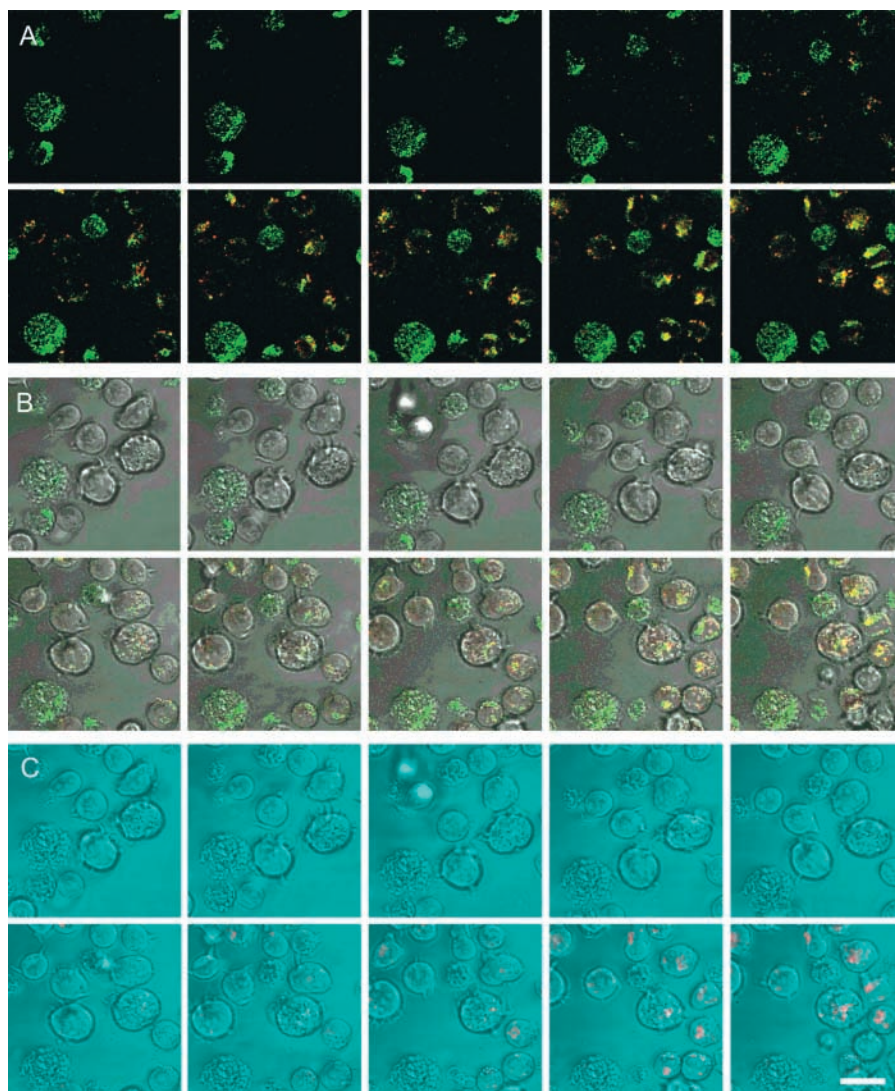
	Intact cells				Permeabilized cells			
	Jurkat cells		Transfected Jurkat cells		Jurkat cells		Transfected Jurkat cells	
	CV	R110	CV	R110	CV	R110	CV	R110
K_m (μ M)	nd ^a	7.5	3.7	10.0	nd	5.8	np ^b	6.2
V_{max} (units ^c)	nd	3516	1743	3857	nd	8530	np	8416

^and, not detectable.

^bnp, not performed.

^cUnits, arbitrary fluorescence units per 4×10^5 cells/ml.

Figure 5 Galleries of confocal images of fluorescence in time in optical sections of CD26/DPPIV-transfected intact living Jurkat cells using 20 μM [Ala-Pro]²-cresyl violet synthetic substrate to localize DPPIV activity. The three galleries are sets of images of the same cells captured at every 30 sec after substrate was added to the incubation medium. (A) Accumulation of [Ala-Pro]²-cresyl violet fluorescence (excitation at 494 μM , emission at 550–580 nm) is shown in green and generation of cresyl violet fluorescence (excitation at 594 nm, emission at >620 nm) in red. Co-localization of substrate and product is shown in yellow. (B) Fluorescence images in A are superimposed on transmission images of cells to demonstrate cellular sites of substrate accumulation and product formation. Note that substrate accumulates especially in cells that do not show product formation. These cells are most likely dead cells. (C) Fluorescence of cresyl violet only is superimposed on transmission images of cells to show exact localization of DPPIV activity. Bar = 20 μm .



transfected Jurkat cells by incubating the cells for 4 min in the presence of both substrates (Figure 4). A small increase in fluorescence over time was observed when both synthetic substrates, but particularly [Ala-Pro]²-cresyl violet, were incubated in the aqueous medium in the absence of cells, indicating spontaneous disintegration of the substrates. The increase in fluorescence over time in wild-type Jurkat cells was similar to the spontaneous disintegration of [Ala-Pro]²-cresyl violet, indicating that other DPPIV-like proteases did not cleave the substrate. CD26/DPPIV-transfected Jurkat cells produced significantly higher amounts of fluorescence at 628 nm in the presence of [Ala-Pro]²-cresyl violet. Figure 4B shows a similar production of fluorescence at 628 nm in intact and permeabilized transfected Jurkat cells against 20 μM [Ala-Pro]²-cresyl violet, again indicating that intracellular DPPIV-like proteases do not cleave the substrate.

Wild-type Jurkat cells lacking CD26/DPPIV process Ala-Pro-rhodamine 110 at a considerable rate, but the reaction velocity in CD26/DPPIV-transfected Jurkat cells against 20 μM Ala-Pro-rhodamine 110 was considerably higher than in Jurkat cells lacking the enzyme (Figure 4C). Permeabilization increases the reaction rate in both wild-type Jurkat cells and transfected Jurkat cells, indicating that intracellular DPPIV-like proteases cleave the rhodamine 110-containing substrate (Figure 4D). Please note that inner filter effects did not play a significant role because all plots are linear with time, showing that saturation does not occur due to inner filter effects. K_m values of cleavage of [Ala-Pro]²-cresyl violet and Ala-Pro-rhodamine 110 by intact living and permeabilized wild-type Jurkat cells and CD26/DPPIV-transfected Jurkat cells were similar in the range of 3–10 μM (Table 1). Remarkably, V_{max} values of Ala-Pro-rhodamine 110 cleavage were

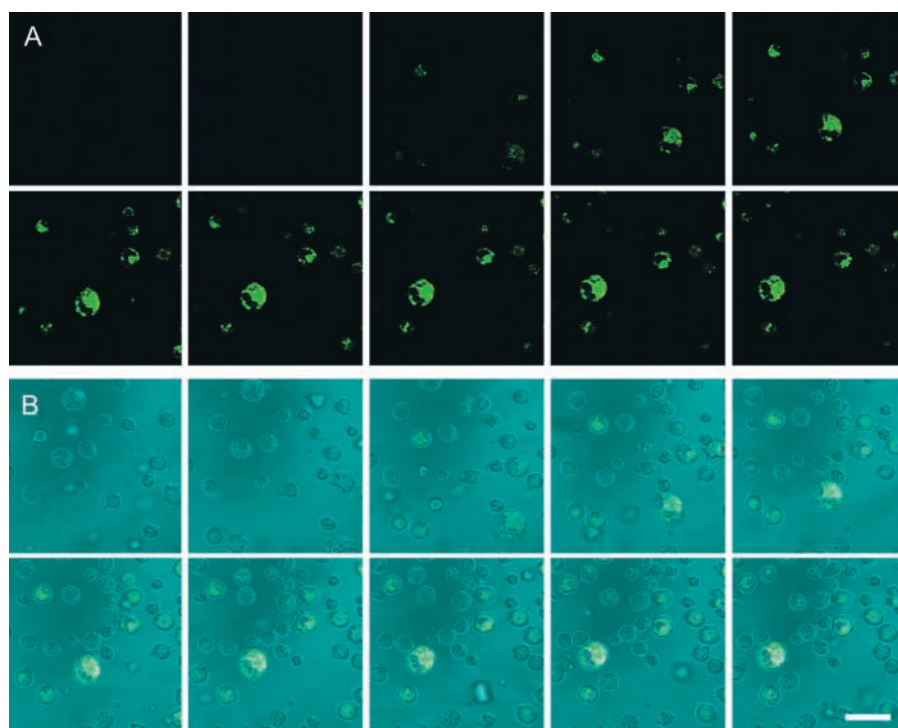


Figure 6 Galleries of confocal images of fluorescence in time in optical sections of intact living Jurkat cells using 20 μM [Ala-Pro]²-cresyl violet synthetic substrate to localize DPPIV activity. The two galleries are sets of images of the same cells captured at every 30 sec after substrate was added to the incubation medium. (A) Same as in Figure 5A. Note that only accumulation of substrate in green is present and formation of product in red or co-localization of substrate and product in yellow are completely absent, indicating that [Ala-Pro]²-cresyl violet is specifically cleaved by DPPIV activity. (B) Fluorescence images in A are superimposed on transmission images of cells to demonstrate cellular sites of substrate accumulation as in Figure 5B, but product formation is completely lacking. Bar = 20 μm .

similar in wild-type Jurkat cells and transfected Jurkat cells, and permeabilization of the cells increased V_{max} almost threefold (Table 1). Please note that V_{max} values are given in arbitrary fluorescence values, so the values for rhodamine 110 can be directly compared but not rhodamine 110 values with cresyl violet values.

Confocal microscopical analysis of cleavage of [Ala-Pro]²-cresyl violet and Ala-Pro-rhodamine 110 in living wild-type Jurkat cells and CD26/DPPIV-transfected Jurkat cells is shown in Figures 5 and 6. Accumulation of cresyl violet in time was observed only in transfected Jurkat cells (Figure 5) and not in Jurkat cells lacking CD26/DPPIV (Figure 6) in small vesicles near the plasma membrane during the first few minutes of incubation. After longer incubation periods, the fluorochrome was transported to other organelles in transfected Jurkat cells (Figure 7), mimicking the pathways of internalization that have been described for CD26/DPPIV (Boonacker and Van Noorden 2003).

When Ala-Pro-rhodamine 110 was used as substrate, fluorescence occurred in both transfected and wild-type living Jurkat cells. Although fluorescence appeared to be more diffuse, accumulation was also observed in small vesicle-like structures near the plasma membrane (Figure 7).

Discussion

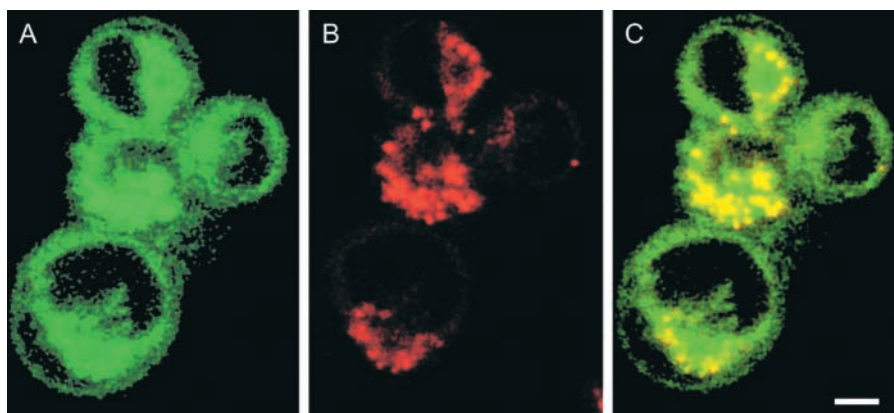
For visualization of specific enzyme reactions in living cells in general and activity of CD26/DPPIV in partic-

ular, it has to be established whether other enzymes interfere in the reaction and whether substrate is available at all sites of the enzyme (Boonacker and Van Noorden 2001). Therefore, we compared synthetic fluorogenic substrates that are considered to be specific for DPPIV activity (Lojda et al. 1976). These synthetic substrates differ in fluorochrome and the number of peptides attached. The rhodamine-containing substrate is monosubstituted, whereas the cresyl violet-containing substrate is bisubstituted.

Surprisingly, the two substrates behaved in rather different ways with respect to specificity. Ala-Pro-rhodamine 110 appeared to react with other DPPIV activity homologues, such as lysosomal DPPII, DPPVIII, and attractin, whereas [Ala-Pro]²-cresyl violet reacted with DPPIV only. The most likely explanation is that the catalytic cleft of DPPIV only is suitable to give access to cresyl violet. The 3D configuration of the tunnel in the molecule of CD26/DPPIV and activity homologues that gives access to the active site is rather tight (Brandt 1997; Gorrell et al. 2000) and must provide steric hindrance for the cresyl violet-based substrate in the DPPIV activity homologues. As both substrates are built up rapidly in T-helper cells, it is unlikely that differences in permeability of the cells for the substrates cause the differentiation in specificity (Boonacker and Van Noorden 2001).

Excitation and emission spectra of cresyl violet and rhodamine 110 are not the same. Therefore, differences in absolute amounts of product formation on the basis of increases in fluorescence cannot be com-

Figure 7 Higher magnification of CD26/DPPIV-transfected intact living Jurkat cells incubated for 5 min in a medium containing 20 μ M [Ala-Pro]²-cresyl violet to demonstrate DPPIV activity. (A) Accumulation of substrate in the cells in green (excitation at 494 nm, emission at 550–580 nm). (B) Product formation in the cells in red (excitation at 594 nm, emission at >620 nm). (C) Combination of images in A and B to show granular intracellular localization of cresyl violet in yellow. Bar = 10 μ m.



pared. Probably, rhodamine 110 is excited more intensely than cresyl violet, because light of 488 nm is more intense than light at 591 nm. The illumination source is not similarly intense throughout the spectrum, as light (lasers) does not produce similar amounts of photons at each wavelength. Furthermore, hydrolysis of monosubstituted and bisubstituted fluorochromes is not comparable either, especially when over 15% of the substrate is hydrolyzed during an assay (Leytus et al. 1983b). Lastly, fluorescence generated during incubation can differ on the basis of the microenvironment of the fluorophore.

With respect to cytotoxicity, it can be stated that low amounts of excitation light should be used to avoid damage to the cells. Preferentially, laser power lower than 10 mW/cm² should be used (E. Manders, personal communication). Illumination by laser light is more toxic for cells containing fluorochromes than cells without fluorochromes. Because of the lower energy of light at longer wavelengths, [Ala-Pro]²-cresyl violet is also to be preferred over Ala-Pro-rhodamine 110 because cresyl violet has to be excited at 591 nm and rhodamine at 488 nm.

A disadvantage of the cresyl violet-based substrate over the rhodamine-based substrate is the rather high instability of the former in aqueous solutions. However, the great advantage of [Ala-Pro]²-cresyl violet is its specificity for DPPIV activity. Wild-type Jurkat cells do not produce more fluorescence than incubation medium only, whereas CD26/DPPIV-transfected Jurkat cells produce distinctly more fluorescence. The same incubations were also performed on permeabilized cells. After sonification, cells were incubated as described above. Permeabilization of wild-type Jurkat cells and of CD26/DPPIV-transfected Jurkat cells did not lead to an additional increase in fluorescence. Apparently, [Ala-Pro]²-cresyl violet does not react with other DPPIV activity homologues.

In intact cells, green fluorescence of the [Ala-Pro]²-

cresyl violet substrate is converted into red fluorescence of the liberated cresyl violet. Strikingly, damaged or apoptotic cells showed hardly any enzymatic activity but did accumulate [Ala-Pro]²-cresyl violet rapidly, as if the enzyme was already inactivated.

Although [Ala-Pro]²-cresyl violet is specific for DPPIV, localization of the cleavage product is another matter. Accumulation of the fluorochrome at first in small submembranous granules and later in larger intracellular compartments may be due to lipophilicity, the charge of cresyl violet, or transport in intact CD26/DPPIV-expressing cells, because intracellular localization patterns are in agreement with the recycling pathway of the M6P receptor, which can bind CD26/DPPIV and molecules associated with it (Boonacker and Van Noorden 2003).

Ala-Pro-rhodamine 110 also shows some spontaneous hydrolysis when dissolved in incubation medium. When incubations were performed with intact living Jurkat cells lacking CD26/DPPIV, hydrolysis of Ala-Pro-rhodamine 110 was distinctly higher, demonstrating its lack of specificity. CD26/DPPIV-positive transfected Jurkat cells produced an additional increase of fluorescence over time. Permeabilization of cells almost doubled the production of fluorescence, indicating that diffusion into the cells of the rhodamine 110-based substrate is a limiting step in the accessibility of this substrate for intracellular proteases other than CD26/DPPIV. Therefore, we conclude that the nature of the fluorophore significantly affects interactions of these synthetic substrates with the active site of DPPIV as has been demonstrated before (Chase and Shaw 1969; Wong and Shaw 1976; Castillo et al. 1979; Lorey et al. 2002).

Acknowledgments

We are grateful to Ms Trees Pierik and Mr Jan Peeterse for careful preparation of the manuscript and figures, respectively.

Literature Cited

- Bleeker FE, Hazen LG, Koehler A, Van Noorden CJF (2000) Direct comparison of the sensitivity of enzyme histochemical and immunohistochemical methods: cathepsin B expression in human colorectal mucosa. *Acta Histochem* 102:247–257
- Boonacker E, Van Noorden CJF (2001) Enzyme cytochemical techniques for metabolic mapping in living cells, with special reference to proteolysis. *J Histochem Cytochem* 49:1473–1486
- Boonacker E, Van Noorden (2002) Determination of reactions of enzymes and their kinetic parameters in living cells by flow cytometry. In Nunez R, ed. *Cytometry: Cytomics, proteomics, genomics*. *Cytometry CD Vol 6*. Multimedia Knowledge, Inc (www.mmke.com) in conjunction with Purdue University Cytometry Labs, New York, 1–8
- Boonacker EP, Van Noorden CJF (2003) The multifunctional or moonlighting protein CD26/DPPIV. *Eur J Cell Biol* 82:53–73
- Brandt W (1997) A molecular model of the active site of dipeptidyl peptidase IV. Explanation of the substrate specificity and interaction with inhibitors. *Adv Exp Med Biol* 421:171–178
- Castillo MJ, Nakajima K, Zimmerman M, Powers JC (1979) Sensitive substrates for human leukocyte and porcine pancreatic elastase: a study of the merits of various chromophoric and fluorogenic leaving groups in assays for serine proteases. *Anal Biochem* 99:53–64
- Chase T Jr, Shaw E (1969) Comparison of the esterase activities of trypsin, plasmin, and thrombin on guanidinobenzoate esters. Titration of the enzymes. *Biochemistry* 8:2212–2224
- Chiravuri M, Schmitz T, Yardley K, Underwood R, Dayal Y, Huber BT (1999) A novel apoptotic pathway in quiescent lymphocytes identified by inhibition of a post-proline cleaving aminodipeptidase: a candidate target protease, quiescent cell proline dipeptidase. *J Immunol* 163:3092–3099
- David F, Bernard AM, Pierres M, Marguet D (1993) Identification of serine 624, aspartic acid 702, and histidine 734 as the catalytic triad residues of mouse dipeptidyl-peptidase IV (CD26). A member of a novel family of nonclassical serine hydrolases. *J Biol Chem* 268:17247–17252
- Demuth H-U, Heins J (1995) Catalytic mechanism of dipeptidyl peptidase IV. In Fleischer B, ed. *Dipeptidyl Peptidase IV (CD26) in Metabolism and the Immune Response*. New York, Springer, 1–35
- Gorrell MD, Abbott CA, Kahne T, Levy MT, Church WB, McCaughan GW (2000) Relating structure to function in the beta-propeller domain of dipeptidyl peptidase IV. Point mutations that influence adenosine deaminase binding, antibody binding and enzyme activity. *Adv Exp Med Biol* 477:89–95
- Hahn K, Touchkine A (2002) Live-cell fluorescent biosensors for activated signaling proteins. *Curr Opin Cell Biol* 14:167–172
- Haugland RP (1995) Detecting enzymatic activity in cells using fluorogenic substrates. *Biotech Histochem* 70:243–251
- Hegen M, Camerini D, Fleischer B (1993a) Function of dipeptidyl peptidase IV (CD26, Tp103) in transfected human T cells. *Cell Immunol* 146:249–260
- Hegen M, Mitrucker HW, Hug R, Demuth HU, Neubert K, Barth A, Fleischer B (1993b) Enzymatic activity of CD26 (dipeptidylpeptidase IV) is not required for its signalling function in T cells. *Immunobiology* 189:483–493
- Hooper JD, Clements JA, Quigley JP, Antalis TM (2001) Type II transmembrane serine proteases. Insights into an emerging class of cell surface proteolytic enzymes. *J Biol Chem* 276:857–860
- Jessani N, Liu Y, Humphrey M, Cravatt BF (2002) Enzyme activity profiles of the secreted and membrane proteome that depict cancer cell invasiveness. *Proc Natl Acad Sci USA* 99:10335–10340
- Jonges GN, Van Noorden CJF, Lamers WH (1992) In situ kinetic parameters of glucose-6-phosphatase in the rat liver lobulus. *J Biol Chem* 267:4878–4881
- Leytus SP, Melhado LL, Mangel WF (1983a) Rhodamine-based compounds as fluorogenic substrates for serine proteinases. *Biochem J* 209:299–307
- Leytus SP, Patterson WL, Mangel WF (1983b) New class of sensitive and selective fluorogenic substrates for serine proteinases. Amino acid and dipeptide derivatives of rhodamine. *Biochem J* 215:253–260
- Lojda Z, Gossrau R, Schiebler TH (1976) *Enzyme Histochemistry. A Laboratory Manual*. New York, Springer, 199–203
- Lorey S, Faust J, Mrestani-Klaus C, Kähne T, Ansoerg S, Neubert K, Bühlung F (2002) Transcellular proteolysis demonstrated by novel cell surface-associated substrates of dipeptidyl peptidase IV (CD26). *J Biol Chem* 277:33170–33177
- Miklos GL, Maleszka R (2001) Protein functions and biological contexts. *Proteomics* 1:169–178
- Patton WF, Beechem JM (2002) Rainbow's end: the quest for multiplexed fluorescence quantitative analysis in proteomics. *Curr Opin Chem Biol* 6:63–69
- Perham RN (2000) Swinging arms and swinging domains in multifunctional enzymes: catalytic machines for multistep reactions. *Annu Rev Biochem* 69:961–1004
- Rawlings ND, Barrett AJ (1996) Dipeptidyl-peptidase II is related to lysosomal Pro-X carboxypeptidase. *Biochim Biophys Acta* 1298:1–3
- Ronquist G, Brody I (1985) The prostasome: its secretion and function in man. *Biochim Biophys Acta* 822:203–218
- Sameni M, Moin K, Sloane BF (2000) Imaging proteolysis by living human breast cancer cells. *Neoplasia* 2:496–504
- Sedo A, Malik R (2001) Dipeptidyl peptidase IV-like molecules: homologous proteins or homologous activities? *Biochim Biophys Acta* 1550:107–116
- Smith AJ, Singhrao SK, Newman GR, Waddington RJ, Embury G (1997) A biochemical and immuno-electron microscopical analysis of chondroitin sulphate-rich proteoglycans in human alveolar bone. *Histochem J* 29:1–9
- Swezey RR, Epel D (1986) Regulation of glucose-6-phosphate dehydrogenase activity in sea urchin eggs by reversible association with cell structural elements. *J Cell Biol* 103:1509–1515
- Tanaka T, Kameoka J, Yaron A, Schlossman SF, Morimoto C (1993) The costimulatory activity of the CD26 antigen requires dipeptidyl peptidase IV enzymatic activity. *Proc Natl Acad Sci USA* 90:4586–4590
- Underwood R, Chiravuri M, Lee H, Schmitz T, Kabcenell AK, Yardley K, Huber BT (1999) Sequence, purification, and cloning of an intracellular serine protease, quiescent cell proline dipeptidase. *J Biol Chem* 274:34053–34058
- Van Noorden CJF (2002) Direct comparison of enzyme histochemical and immunohistochemical methods to localize an enzyme. *Mar Environ Res* 54:575–577
- Van Noorden CJF, Bahns S, Koehler A (1997a) Adaptational changes in kinetic parameters of G6PDH but not of PGDH during contamination-induced carcinogenesis in livers of North Sea flatfish. *Biochim Biophys Acta* 1342:141–148
- Van Noorden CJF, Boonacker E, Bissell ER, Meijer AJ, van Marle J, Smith RE (1997b) Ala-Pro-cresyl violet, a synthetic fluorogenic substrate for the analysis of kinetic parameters of dipeptidyl peptidase IV (CD26) in individual living rat hepatocytes. *Anal Biochem* 252:71–77
- Van Noorden CJF, Frederiks WM (1992) *Enzyme Histochemistry. A Laboratory Manual of Current Methods*. Oxford, BIOS, 90–91
- Wong SC, Shaw E (1976) Inactivation of trypsin-like proteases by active-site-directed sulfonylation. Ability of the departing group to confer selectivity. *Arch Biochem Biophys* 176:113–118
- Yaron A, Naider F (1993) Proline-dependent structural and biological properties of peptides and proteins. *Crit Rev Biochem Mol Biol* 28:31–81